Proceedings of Symposium on Ultrasonic Electronics, Vol. 34 (2013) pp. 91-92
20-22 November, 2013

Evaluation of crack closure stress by damped double nodes analyses of images obtained by global preheating and local cooling

広域加熱・局所冷却を用いた閉じたき裂の映像の減衰二重節点解析による閉口応力の評価

Koji Takahashi[1†], Kentaro Jinno[1], Yoshikazu Ohara[1] and Kazushi Yamanaka[1] ([1]Tohoku Univ.)
高橋　恒二[1†]，神納　健太郎[1]，小原　良和[1]，山中　一司[1]([1]東北大)

1. Introduction

To measure closed crack depths without underestimation, we have developed an imaging method, the subharmonic phased array for crack evaluation (SPACE).[1)] However, when short burst input waves are used to obtain a high temporal resolution, strong linear scatterers appear in subharmonic images due to spectrum broadening. This degrades the selectivity of closed crack.

To solve this problem, we have developed a load difference phased array (LDPA), [2)] based on the subtraction between images at different loads. As a practical method for applying a load to cracks, the use of thermal stress induced by local cooling (LC) with a cooling spray has been studied.[3)] However, the thermal stress is insufficient to open tightly closed crack owing to the limited cooling temperature determined by each cooling medium. Then, as a method for opening tightly closed crack, we proposed global preheating and local cooling (GPLC) and demonstrated its validity and high selectivity imaging of closed crack combining with LDPA.[4)] However, the thermal stress induced by GPLC and crack closure stress has not been examined. Relationship between the changes in PA images and the opening/closing state of cracks has also not been examined in detail.

In this study, we estimate the thermal stress based on heat transfer analysis and propose a method of estimating crack closure stress. Furthermore, we compare PA images obtained by simulation using damped double node (DDN) model[5)] with those obtained in the experiments.

2. Experimental conditions

In this experiment, we used a compact tension (CT) specimen (A7075) with closed fatigue crack with a depth of 11.3 mm.[4)] In GPLC, after heating the specimen to 323 K by a hotplate, the top surface of the specimen was cooled by two cooling sprays (−218 K) for 10 s. At the same time, we imaged cracks by PZT array transducer (5 MHz、32 el.) and PA (Fig. 1).

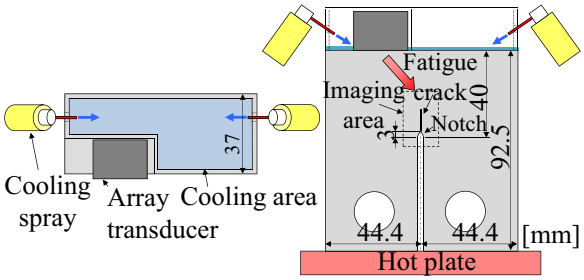

Fig. 1 Experimental configuration.

3.Experimental results

The PA images obtained by GPLC are shown in Fig. 2. After GP and before LC, the closed crack was not imaged in Fig. 2(a). On the other hand, at a time t=2 s after the onset of LC, the crack was observed and the depth was 8.7 mm in Fig. 2(b). At t=4 s, the maximum crack depth of 11.3 mm was observed in Fig. 2(c). This is the same as the actual crack depth of 11.3 mm observed by applying a tensile load.[4)] This result shows that GPLC is significantly effective in opening a tightly closed crack.

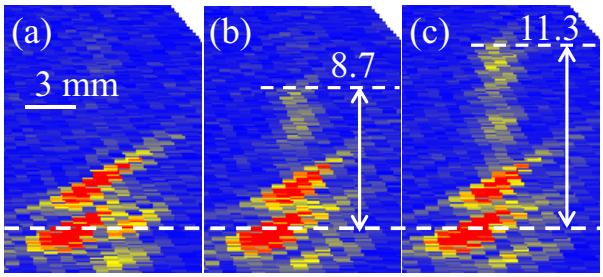

Fig. 2 PA images during GPLC: (a)Before LC, (b)t=2 s, (c)t=4 s.

4. Analysis of thermal stress induced by GPLC

To examine the thermal stress induced by GPLC, we analyzed it by 1D heat transfer analysis. Assuming the boundary condition of the third kind at the top surface and semi-infinite solid, the thermal stress within the specimen $T(z,t)$ is given by[6)]

$$T(z,t)=(T_\infty-T_i)\{erfc(\frac{z}{2\sqrt{\alpha t}}) - \exp(\frac{hz}{k}+\frac{h^2\alpha t}{k^2})erfc(\frac{z}{2\sqrt{\alpha t}}+\frac{h\sqrt{\alpha t}}{k})\}+T_i \quad (1)$$

where T_∞ is the cooling temperature due to LC, T_i is the initial temperature due to GP, k is the thermal conductivity, h is the heat transfer coefficient, α is the thermal diffusivity. The thermal bending stress is given by[7]

$$\sigma(z,t)=\frac{12\alpha Ez}{H^3(1-\nu)}\int_{-\frac{H}{2}}^{\frac{H}{2}}T(z,t)dz\,. \quad (2)$$

Assuming that thermal stress acting on the top surface of the specimen is the maximum bending stress σ_{max}, we estimated σ_{max} using the parameters listed in Table 1. We compared this with the crack depth d in PA images in Fig. 3. As a result, σ_{max} took a peak at t =4-6 s and σ_{max} gradually decreased t >6 s. Therefore, we could explain the experimental result by the analysis of thermal stress. Assuming the crack was completely opened at t =4 s, the thermal stress can be regarded as crack closure stress. Then we estimated that the crack closure stress intensity factor is

$K_C \approx 17.9\ \mathrm{MPa}\sqrt{\mathrm{m}}$ ($\sigma_C \approx 95\ \mathrm{MPa}$).

Table 1 Parameters used for analysis[8]

T_∞ [K]	T_i [K]	h [W/(m^2・K)]	k [W/(m・K)]	α [m^2/s]
218	323	1.5×10^4	130	8.4×10^{-5}

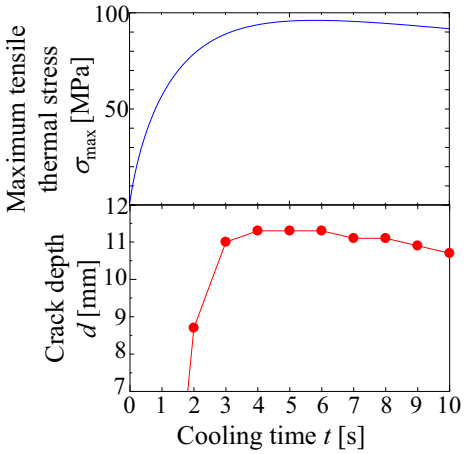

Fig. 3 Comparison between analyzed thermal stress and the crack depths in PA image: (a) Maximum thermal stress σ_{max}, (b) Crack depth d.

5. Simulations by DDN model

To examine the changes of experimental PA images and the opened and closed state of cracks in detail, we simulated by DDN models.[5] Here, we simulated the specimen used in the experiment. Input waves (40 nm, 5 MHz, 3 cycles) were focused on the middle part of crack.

Snapshots and PA images obtained by the simulations are shown in Figs. 4 and 5, respectively. At t =0 s, the scattered waves from only notch was observed in Figs 4(a) and 5(a). On the other hand, at t =2 s, the scattered waves from notch and the middle part of crack were observed in Figs. 4(b) and 5(b). At t =4 s, the scattered waves from notch and the crack tip were observed in Figs. 4(c) and 5(c). This is because the thermal stress acting on the crack increased and the crack was opened as t increased. Thus, the experimental results were successfully reproduced by the simulation.

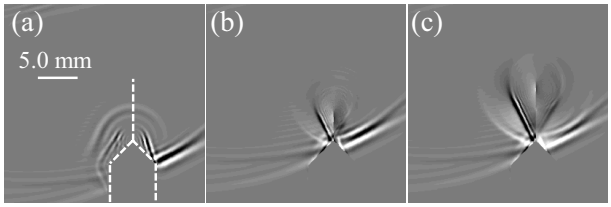

Fig. 4 Snapshots by simulation: (a)t=0 s, (b)t=2 s, (c)t=4 s.

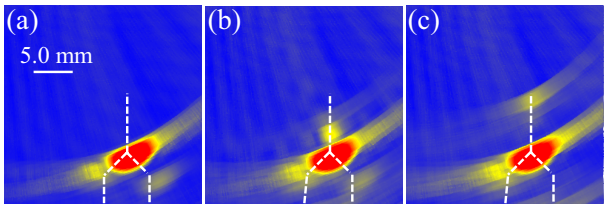

Fig. 5 PA images by simulation: (a)t=0 s, (b)t=2 s, (c)t=4 s.

6. Conclusions

We proposed the thermal stress induced by GPLC and estimated the crack closure stress by the heat transfer analysis and the equation of thermal bending stress. The tendency of the phased array image was reproduced by simulations with the DDN model incorporating the thermal stress.

References

1) Y. Ohara, T. Mihara, R. Sasaki, T. Ogata, S. Yamamoto, Y. Kishimoto, K. Yamanaka, Appl. Phys. Lett, **90** (2007) 011902.
2) Y. Ohara, S. Horinouchi, M. Hashimoto, Y. Shintaku, K. Yamanaka, Ultrasonics, **51** (2011) 661.
3) P. B. Nagy, G. Blaho, Rev. Prog. QNDE, **14** (1995) 1979.
4) Y. Ohara, K. Takahashi, S. Murai, K. Yamanaka, Appl. Phys. Lett., **103** (2013) 031917.
5) K. Yamanaka, Y. Ohara, M. Oguma, Y. Shintaku, Appl. Phys. Express., **4** (2011) 076601.
6) F. P. Incropera, D. P. D. Witt, Introduction to Heat Transfer (1990) 286.
7) S. P. Timoshenko, J. N. Goodier, Theory of Elasticity (1990) 403.
8) E. A. Brandes, G. B. Brook, Smithells Metals Reference Book (1992) 129.